Title

Targeted Proteomic Analysis of Small GTPases in Murine Adipogenesis.

Journal

Analytical Chemistry, 92(9)

Authors

Yang, Yen-Yu
Huang, Ming
Wang, Yinsheng

Publication Date

2020-05-05

DOI

10.1021/acs.analchem.0c00974

Peer reviewed

Published in final edited form as:

Anal Chem. 2020 May 05; 92(9): 6756–6763. doi:10.1021/acs.analchem.0c00974.

Targeted Proteomic Analysis of Small GTPases in Murine Adipogenesis

Yen-Yu Yang

Department of Chemistry, University of California, Riverside, California 92521-0403, United States

Ming Huang

Environmental Toxicology Graduate Program, University of California, Riverside, California 92521-0403, United States

Yinsheng Wang

Department of Chemistry and Environmental Toxicology Graduate Program, University of California, Riverside, California 92521-0403, United States

Abstract

Small GTPases are essential signaling molecules for regulating glucose uptake in adipose tissues upon insulin stimulation, and this regulation maintains an appropriate range of glycemia. The involvement of small GTPases in adipogenesis, however, has not been systemically investigated. In this study, we applied a high-throughput scheduled multiple-reaction monitoring (MRM) method, along with the use of synthetic stable isotope-labeled peptides, to identify differentially expressed small GTPase proteins during adipogenesis of cultured murine cells. We were able to quantify the relative levels of expression of 55 and 49 small GTPases accompanied by adipogenic differentiation in 3T3-L1 and C3H10T1/2 cells, respectively. When compared with analysis conducted in the data-dependent acquisition (DDA) mode, the MRM-based proteomic platform substantially increased the coverage of the small GTPase proteome. Western blot analysis further corroborated the MRM quantification results for selected small GTPases. Interestingly, overall a significant number of small GTPases were down-regulated during adipogenesis. Among them, the expression levels of Rab32 protein were consistently lower in differentiated adipocytes than the corresponding undifferentiated precursors in both cell lines. Overexpression of Rab32 in 3T3-L1 and C3H10T1/2 cells prior to adipogenesis induction suppressed their differentiation. Together, this is the first comprehensive analysis of the alterations in small GTPase proteome during adipogenesis, and we reveal a previously unrecognized role of Rab32 in adipogenic differentiation.

Corresponding Author: Yinsheng Wang - Department of Chemistry and Environmental Toxicology Graduate Program, University of California, Riverside, California 92521-0403, United States; yinsheng.wang@ucr.edu.

The authors declare no competing financial interest.

Supporting Information

The Supporting Information is available free of charge at https://pubs.acs.org/doi/10.1021/acs.analchem.0c00974.

Venn diagrams and bar graphs showing the quantification results of small GTPase proteins during differentiation of precursor cells to adipocytes (PDF)

Excel file containing the processed quantification data (XLSX)

Complete contact information is available at: https://pubs.acs.org/10.1021/acs.analchem.0c00974

Graphical Abstract

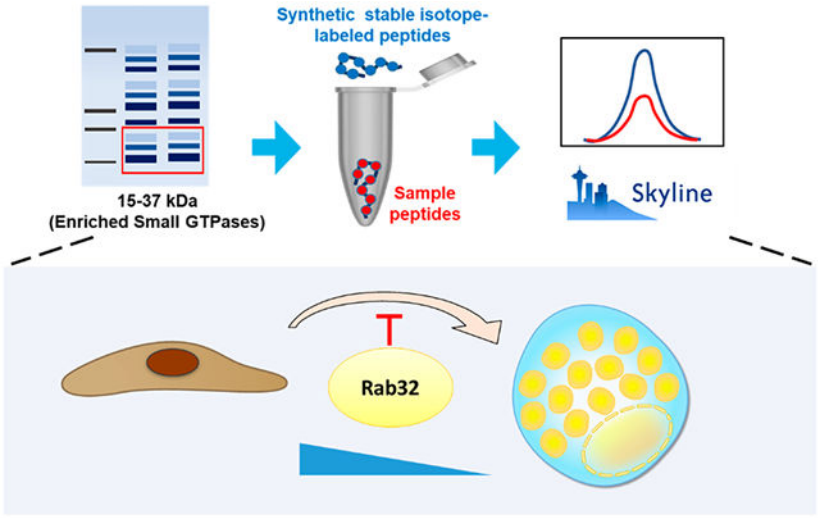

Adipocytes play a crucial role in energy homeostasis, not only passively serving as the primary energy depot, but also actively participating in various physiological processes that regulate metabolism.[1] However, excessive adiposity, or obesity, is a major risk factor for metabolic syndromes, which is manifested by the observation that overweight patients are often comorbid with type 2 diabetes, hyperlipidemia, and cardiovascular diseases.[2–4] Epidemiological studies also identified obesity as a significant risk factor for various cancers.[5,6] A recent report from the World Health Organization shows that globally more than 1.9 billion adults are overweight or obese, and such high prevalence poses a great threat to worldwide public health.[7] Thus, unveiling novel adipogenic pathways may provide a molecular basis for targeting the primary risk factors for these prevalent noncommunicable diseases.

Adipogenesis is a strictly regulated process under the control of multiple intrinsic and extrinsic factors.[8] The precursor stem cells first commit into a transitional stage called preadipocytes, which lose their multipotent potential. Later, the preadipocytes enter the final stage of adipogenesis and start expressing adipocyte-specific genes to activate the machinery for lipid synthesis and storage.[8] Current research in the molecular regulation of adipogenesis focuses on transcriptional activation of adipocytic genes by peroxisome proliferator-activated receptor γ (PPAR-γ), CCAAT-enhancer-binding proteins (C/EBPs), and Krüppel-like factors (KLFs).[9] However, the upstream regulation and signal transduction cascades for these nuclear transcription factors remain largely unexplored. Previous studies also documented that adipogenesis induction by 3-isobutyl-1-methyl xanthine (IBMX) leads to the accumulation of cyclic adenosine monophosphate (cAMP), thereby activating protein kinase A (PKA). Nevertheless, not much is known about the downstream proteins involved in this adipogenic signaling cascade.[10]

Interestingly, previous studies have shown that some small GTPases assume important roles in PKA-mediated adipogenic differentiation.[11] Small GTPases are monomeric guanine nucleotide-binding proteins that comprise several subfamilies, including Ras, Rab, Rho, Arf,

and Ran.[12] In response to environmental stimulation such as hormones, these proteins function as pivotal hubs of various cellular processes, including cell division, differentiation, and signal transduction.[13–16]

Several small GTPases have been previously characterized in adipocytes. For instance, Arl15 mediates metabolic regulation in adipose tissues[17] and the Rho subfamily was found to be involved in adipogenesis.[18,19] Nevertheless, there has been no comprehensive analysis about the entire superfamily of small GTPases in regulating adipogenesis and adipocyte physiology.

We recently developed a targeted proteomic method for interrogating the small GTPase proteome,[20,21] which exploits their narrow molecular weight distribution (15–37 kDa) for their enrichment by SDS-PAGE followed by in-gel digestion of the enriched proteins. In this study, we employed this method, in conjunction with scheduled multiple-reaction monitoring (MRM) and synthetic stable isotope-labeled peptides, to assess the altered protein expression of small GTPases accompanied by adipogenic differentiation. We observed overall diminished expression of a large number of small GTPases and uncovered a previously unknown role of Rab32 in suppressing adipogenesis.

EXPERIMENTAL SECTION

Cell Culture and Adipocyte Differentiation.

3T3-L1 murine preadipocyte (ATCC CL-173) and C3H10T1/2 murine mesenchymal stem cells (MSC; ATCC CCL-226) were cultured in Dulbecco's modified Eagle's medium (DMEM) supplemented with 10% newborn calf serum (Gibco) and fetal bovine serum (Fisher), respectively, and penicillin/streptomycin (100 IU/mL, GE Healthcare). Both lines of cells were subcultured at 80% confluence and maintained in a humidified atmosphere containing 5% CO_2. All experiments were conducted within 25 and 15 passages for 3T3-L1 and C3H10T1/2 cells, respectively.

Adipogenesis was induced as described previously.[22,23] Briefly, differentiation was initiated at 2 days postconfluence in complete DMEM containing 1 μM dexamethasone (Sigma), 0.5 mM 3-isobutyl-1-methylxanthine (Sigma), and 175 nM (for 3T3-L1 cells) or 1750 nM (for C3H10T1/2 cells) insulin (Sigma). After 48 h, the cells were refreshed with maintenance medium containing complete DMEM and 10 nM insulin. Maintenance medium was changed in every 48 h and the cells were harvested for protein extraction at 96 h postdifferentiation. For overexpression, approximately 1.5×10^6 cells in a 6-well plate were first transiently transfected with 1.5 μg of plasmid encoding human RAB32 (Addgene plasmid #49611) using transIT-2020 (Mirus mir5400), and adipogenesis was induced 48 h later.

Cell Lysis and Protein Digestion.

Cells were trypsinized and washed once with phosphate-buffered saline (PBS). Total proteins were extracted by incubating with CelLytic M cell lysis reagent (Sigma) containing 1% protease inhibitor cocktail (Sigma) on-ice for 30 min, followed by centrifugation at 16000 *g* for 30 min at 4 °C. Lysates were transferred into a prechilled tube by using a 1 mL

syringe with a 26G needle without disturbing the floating lipid layer. Protein concentrations were determined by Quick Start Bradford Protein Assay (Bio-Rad).

For LC-MRM analysis, the cell lysates were concentrated with a 10 kDa MWCO centrifugal filter (VWR), and 100 μg of protein was mixed with 4× Laemmli SDS loading buffer to a final volume of 40 μL. Total proteins were resolved using a 10% SDS-PAGE gel and stained with Coomassie Brilliant Blue R-250. Gel bands in the molecular weight range of 15–37 kDa were excised for tryptic digestion. Briefly, the gel was cut into 1 mm^3 cubes and destained sequentially with 25% and 50% acetonitrile (ACN) in 50 mM ammonium bicarbonate (pH 7.8). The proteins were subjected to reduction with 10 mM dithiothreitol (DTT) at 37 °C for 1 h and alkylation with 55 mM iodoacetamide at room temperature in dark for 20 min. The proteins were then digested in-gel with trypsin at 37 °C for 18 h with an enzyme/protein ratio of 1:100. Peptides were extracted from the gel pieces with 50% ACN/5% acetic acid (HOAc), concentrated by Speed-Vac and desalted by using C18 ZipTip (Agilent). A crude pool of synthetic small GTPase peptides (New England Peptide, Inc.) with a C-terminal [$^{15}N_2$, $^{13}C_6$]-labeled lysine (+8.0 Da) or [$^{15}N_4$, $^{13}C_6$]-labeled arginine (+10 Da) (~4.0 fmol each) were spiked into approximately 4% of the digestion mixture, and the resulting mixture was subjected to LC-MRM analysis.[24]

Liquid Chromatography-Tandem Mass Spectrometry (LC-MS/MS).

LC-MS/MS experiments were conducted on a TSQ Altis triple-quadrupole mass spectrometer operated in the MRM mode or an Q Exactive Plus hybrid quadrupole-Orbitrap mass spectrometer operated in the DDA mode. Peptides were separated with an UltiMate 3000 UPLC (Thermo Fisher Scientific, San Jose, CA) prior to electrospray ionization. Peptide mixtures were loaded onto a 4 cm capillary column (150 μm i.d.) packed with C18 resin (5 μm in particle size and 120 Å in pore size, Dr. Maisch GmbH HPLC) at a flow rate of 3 μL/min. The peptides were separated on a ~25 cm analytical column (75 μm i.d.) packed with C18 resin (3 μm in particle size and 120 Å in pore size, Dr. Maisch GmbH HPLC) with a 90-min gradient of 2–35% ACN in 0.1% formic acid at a flow rate of 300 nL/min. Ions were isolated with an FWHM of 0.7 in both Q1 and Q3 with a cycle time of 3 s. The collision energies for fragmenting the precursor ions were based on the default setting in Skyline.[25]

An MRM library for 138 unique peptides derived from murine small GTPases was generated with Skyline using LCMS/MS data acquired from shotgun proteomic analyses.[21,24] The precursor → product ion transitions were monitored in a 3 min retention time window converted from its normalized retention time (iRT) and the iRT-RT standard curve of 10 standard peptides from the tryptic digestion mixture of BSA.[26] All targeted peptides were manually inspected and filtered at dot-product (dotp) > 0.7 to ensure that the peak was correctly picked for the transitions. The relative levels of the targeted peptides were calculated from the ratios of sum of peak areas for the transitions of sample over the corresponding heavy stable isotope-labeled peptides. Each sample was analyzed twice, and the values from the two technical replicates were averaged to represent one biological replicate. A total of two and three biological replicates were conducted for 3T3-L1 and C3H10T1/2 cells, respectively.

Oil Red O Staining.

Oil Red O staining was performed as described previously.[27] Briefly, cells were washed once with PBS and fixed in 3.7% formaldehyde in PBS at room temperature for 1 h. The fixed cells were stained with 3 mg/mL Oil Red O (Sigma) in 60% isopropanol at room temperature for 30 min. Excess dye was subsequently washed off with water. Bright field images were recorded with a BZX710 Automated Microscope (Keyence).

RNA Extraction and Real-time Quantitative-PCR (RT-qPCR).

Total RNA was extracted with Total RNA Kit I (Omega) and purified with HiBind RNA mini columns (VWR). cDNA was generated from 1 μg of total RNA. Approximately 66 ng of cDNA was mixed with Luna qPCR master mixture (New England Biolabs) in a 96-well optical reaction plate and the reaction was monitored with Biorad CFX Connect. The primer sequences used for qPCR were Rab32 forward, TACGTGCACCAGCTCTTCTCC; Rab32 reverse, TCGAGTCATGTTGCCAAACCG; PPARγ forward, CGCTGATGCACTGCCTATGA; PPARγ reverse, AGAGGTCCACAGAGCTGATTCC; GAPDH forward, CATCACTGCCACCCGAAGACTG; GAPDH reverse, ATGCCAGTGAGCTTCCCGTTCAG.

RESULTS

Scheduled MRM Profiling of Differentially Expressed Small GTPases During Adipogenic Differentiation.

Augmented adipogenesis contributes to metabolic diseases such as obesity and diabetes, yet the proteins factors involved in adipocyte differentiation from mesenchymal stem cells remain largely unexplored. In the present study, we aim to systemically characterize the alterations in expression of small GTPase proteins from adipose-derived stem cells that have committed to the adipocyte lineage. To improve the coverage of the small GTPase proteome and the throughput of the method, we employed scheduled MRM analysis coupled with gel fractionation (Figure 1).[20] The high-throughput of the method is reflected by the fact that we were able to monitor 138 small GTPases, which represent approximately 80% of the murine small GTPase proteome,[28] in a single 90 min LC-MS/MS run. The method is capitalized on the fact that the molecular weights of most small GTPases are in the range of 15–37 kDa; thus, we enriched the small GTPase proteome using SDS-PAGE and excised the gel bands in the corresponding molecular weight range.

To achieve sensitive and reliable detection of small GTPase peptides, we selected one unique peptide for each small GTPase in our library and chose the three most abundant y-ions for each peptide based on MS/MS acquired from shotgun proteomic analyses. Together, we incorporated peptides derived from 138 murine small GTPases into our Skyline MRM library (Figure S1). Prior to injection, the samples were mixed with the synthetic stable isotope-labeled heavy peptides of identical amino acid sequences to our target analytes. It is noteworthy that the heavy peptides and the unlabeled sample peptides had nearly identical retention times and thus they were ionized at the same time. In LC-MRM analyses, the mass spectrometer was scheduled to monitor a subset of transitions in a predefined 3 min retention time window calculated from an iRT algorithm.[26]

3T3-L1 murine embryonic fibroblastic cells and C3H10T1/2 murine mesenchymal stem cells (MSC) are pluripotent stem cells that can be differentiated into a subset of cell types including adipocyte.[29–31] Numerous pivotal metabolic networks, for example, the molecular regulation of glucose uptake upon insulin stimulation, have been discovered in adipocytes derived from these two cell lines.[23,32,33] Thus, these cell lines are ideal systems to reveal the molecular determinants of adipogenic differentiation. Herein, we induced the differentiation of 3T3-L1 and C3H10T1/2 cells into adipocytes, and the differentiation efficiency was quantified by Oil Red O staining (Figure 2A). Notably, while the majority of 3T3-L1 fibroblasts were almost fully differentiated into adipocytes, the differentiation efficiency for C3H10T1/2 cells was only approximately 20%, with the rest being undifferentiated precursor cells, which is consistent with the previous findings.[23]

A total of 100 μg of protein lysate was separated by SDS-PAGE, and the 15–37 kDa protein fraction was digested in-gel with trypsin. Approximately 4% of the ensuing digestion mixture was injected for LC-MS/MS analysis. Together, we quantified 55 and 49 small GTPases in 3T3-L1 and C3H10T1/2 cells, respectively, and among them 41 were commonly detected in both cell lines (Figures 2B,C, S1, and S2). To evaluate the sensitivity of the scheduled MRM method, we also analyzed the same samples in data-dependent acquisition (DDA) mode. In DDA mode, precursor ions for acquiring MS/MS are selected on the basis of their relative abundances, which leads to inherently poor reproducibility in the identification and quantification of low-abundance coeluting peptides. In contrast, MRM selectively monitors the peptides of interest and thus increases the detection sensitivity and reproducibility. Indeed, our results showed that the scheduled MRM analysis provides ~8- and 11-fold increases in total numbers of quantified small GTPases in 3T3-L1 and C3H10T1/2 cells, respectively, as compared with DDA analysis (Figure S3).

Interestingly, we found an overall diminished expression of small GTPases upon differentiation to adipocytes (Figure 3A,B). Rho small GTPases are by far the most well characterized family of small GTPases in adipogenesis. Excessive activities of Rho GTPases (e.g., RhoA) redirects the differentiation of precursor stem cells and inhibits adipogenesis,[18] and RhoA also promotes osteogenesis while suppressing adipogenesis.[19] Our results revealed decreased expression of RhoC in both cell lines and RhoA in 3T3-L1 upon differentiation to adipocytes. Hence, suppressing the activities or protein expressions of certain small GTPases might be crucial for adipogenic differentiation from mesenchymal stem cells.

Validation of Differentially Expressed Small GTPases with Western Blot Analysis.

Our proteomic results revealed an overall down-regulation of small GTPases during adipogenesis. To determine the key regulators that orchestrate adipogenic differentiation, we applied a cutoff of 1.5-fold change and found that, among all the quantified small GTPases, 2 and 35 proteins were up- and down-regulated, respectively, in 3T3-L1 cells (Figure S4A,B). In contrast, only six small GTPases were found decreased with the same threshold in C3H10T1/2 cells (Figure S4B), which can be rationalized from the relatively low differentiation rate of this cell line (Figure 2A). As the majority of the C3H10T1/2 cells remained undifferentiated, we can expect a higher background in discovering the

differentially expressed small GTPases accompanied by adipogenesis. In this regard, by lowering the cutoff threshold to 1.3-fold for C3H10T1/2 cells, we were able to identify 17 small GTPases exhibited differential expression, and 13 out of these 17 proteins were also down-regulated in 3T3-L1 cells upon differentiation into adipocytes (Figure S5).

Strikingly, we observed larger alterations in quantification results for the expression levels of small GTPases from C3H10T1/2 than 3T3-L1 cells (Table S1). This can be attributed to the greater heterogeneity of C3H10T1/2 cells.[34] As a result, the C3H10T/2 cells are more multipotent with respect to cell differentiation. This variability is also highlighted by the advice that C3H10T1/2 cells are cultured within 15 passages,[35,36] suggesting that the cell physiology might drift progressively in later passages.

Although the two precursor cell lines employed for the adipogenic differentiation differ from each other in various physiological aspects, we expect that general regulatory small GTPases will exhibit similar trends in expression levels upon differentiation. Indeed, a comparison of the data from the two cell lines showed that Rab32 was consistently down-regulated in adipocytes relative to their precursor stem cells. To further confirm the findings made from the scheduled MRM analysis, we employed Western blot analysis for several small GTPases using commercially available antibodies (Figure 4A,B). The Western blot results confirmed the quantification data obtained from MRM analysis, thereby supporting the accuracy and robustness of scheduled MRM in quantifying the alterations in expression levels of small GTPases during adipogenic differentiation.

Rab32 is a Novel Suppressor of Adipogenesis.

Previous studies revealed Rab32 as an important regulator for metabolism, where cells expressing Rab32 dominant-negative mutants failed to accumulate lipid droplets.[37] Results from our scheduled MRM analysis prompted us to posit that diminished expression of Rab32 may promote adipogenic differentiation. To test this hypothesis, we overexpressed Rab32 in 3T3-L1 and C3H10T1/2 cells. The degree of differentiation was again examined with Oil Red O staining and the results demonstrated that augmented expression of Rab32 significantly suppressed adipogenesis in both lines of cells (Figure 5A,B).

While the protein level of Rab32 decreased upon differentiation, the molecular mechanism through which it is down-regulated during differentiation remains unclear. To further investigate the regulation of Rab32 expression, we used real-time PCR to assess the changes in mRNA level of Rab32 during differentiation of C3H10T1/2 cells. Our results showed that, while the mRNA level of the master driver for adipocyte differentiation, that is, PPARγ, was increased, manifesting a successful induction, the differentiation did not alter the mRNA expression level of Rab32 (Figure S6). Thus, the precursor stem cells may orchestrate attenuated Rab32 expression via a post-transcriptional mechanism.

DISCUSSION

To our knowledge, this is the first scheduled LC-MRM, coupled with synthetic stable isotope-labeled peptides, for the quantitative analysis of differential expression of the murine small GTPase proteome. With the high-throughput method presented herein, we were able to

accurately quantify 55 and 49 small GTPases in 3T3-L1 and C3H10T1/2 cells, respectively, upon differentiation into adipocytes. To evaluate the performance of the MRM method, we also performed DDA analysis for the same tryptic peptide mixtures, and the results demonstrated that scheduled MRM afforded superior reproducibility and sensitivity in the quantitative assessment of the small GTPase proteome.[38,39] Notably, Huang et al.,[20,21,40] by employing a similar approach with stable isotope labeling by amino acids in cell culture (SILAC) technique, successfully quantified approximately 90 small GTPases in human cells, which offered significantly increased coverage of small GTPase proteome when compared to analysis conducted in the DDA mode. In this vein, while DDA mode is commonly used in exploratory proteomic analysis, targeted proteomics such as MRM can provide more sensitive and reproducible quantification for a subset of proteins of interest such as disease biomarkers.[41,42] Together, we demonstrated a reliable and efficient platform in revealing differential expression of small GTPases in cultured murine cells. It is noteworthy that the heavy isotope-labeled peptides were spiked into the samples prior to injection for LC-MS/MS analyses, which shows the adaptability and flexibility of the method to any specimens that are not amenable to metabolic labeling, e.g. clinical samples.[24]

To date, the involvement of small GTPases in cell fate determination in adipogenesis remains largely unexplored. Here, we systemically examined the differential expression of the small GTPase proteome during adipogenesis. Our results validated that the known suppressors for adipogenesis, that is, the Rho family small GTPases (e.g., RhoA), were down-regulated upon adipogenesis.[18,43] Among the quantified small GTPases, we found that the expression of Rab32 was consistently lower in the differentiated adipocytes relative to the undifferentiated precursor cells. Functionally, Rab32 is a known regulatory factor in lipid accumulation. Dominant-negative Rab32 mutation prevents lipid droplet formation in fruit flies.[37,44] Although Rab32 is known to modulate lipid metabolism, its role in adipogenesis has not yet been characterized. Here, we found that Rab32 may negatively regulate adipogenesis, as overexpression of Rab32 suppresses the adipogenic differentiation of 3T3-L1 and C3H10T1/2 cells.

Rab32 was shown to interact with protein kinase A (PKA) and regulate intracellular transport of vesicles in a cAMP-dependent manner.[45,46] Interestingly, the same pathway can be activated by a phosphodiesterase inhibitor IBMX,[47] a component of the adipogenesis induction cocktail used herein. Such activation of the cAMP/PKA pathway leads to the expression of adipogenesis driver, PPARγ, thereby orchestrating the differentiation of mesenchymal stem cells toward adipocytes. Thus, Rab32 may mediate adipogenesis via PKA, though the underlying mechanism awaits further study.

Our real-time PCR results showed that during adipogenesis, while Rab32 protein levels were down-regulated after induction of adipogenesis, its mRNA levels remained unchanged. Our findings suggested that attenuated level of Rab32 protein during adipocyte differentiation may arise from a yet-to-be-identified factor that suppresses Rab32 translation via a RNA modification-dependent mechanism.[48,49]

In conclusion, we have demonstrated the accuracy and sensitivity of the scheduled MRM method in studying differentially expressed small GTPases in murine cells. Our results

showed that the method allowed for high-throughput detection of small GTPase proteins in murine cells. With the method, we discovered approximately 20 candidate small GTPase regulators of adipogenesis. In addition, we documented Rab32 as a suppressor for adipogenic differentiation. To our knowledge, this is the first comprehensive study of the reprogramming of the small GTPases during adipogenesis.

Supplementary Material

Refer to Web version on PubMed Central for supplementary material.

ACKNOWLEDGMENTS

The authors would like to thank Prof. Alan Saltiel and Shaochen Chen at the University of California San Diego for providing the 3T3-L1 and C3H10T1/2 cells, respectively.

Funding

This work was supported by the National Institutes of Health (R01 CA210072).

REFERENCES

(1). Rosen ED; Spiegelman BM Nature 2006, 444, 847–53. [PubMed: 17167472]

(2). Lavie CJ; Milani RV; Ventura HO J. Am. Coll. Cardiol 2009, 53, 1925–32. [PubMed: 19460605]

(3). Jeffery E; Church CD; Holtrup B; Colman L; Rodeheffer MS Nat. Cell Biol 2015, 17, 376–85. [PubMed: 25730471]

(4). Bhupathiraju SN; Hu FB Circ. Res 2016, 118, 1723–35. [PubMed: 27230638]

(5). van Kruijsdijk RC; van der Wall E; Visseren FL Cancer Epidemiol., Biomarkers Prev 2009, 18, 2569–78. [PubMed: 19755644]

(6). Yoshimoto S; Loo TM; Atarashi K; Kanda H; Sato S; Oyadomari S; Iwakura Y; Oshima K; Morita H; Hattori M; Honda K; Ishikawa Y; Hara E; Ohtani N Nature 2013, 499, 97–101. [PubMed: 23803760]

(7). Swinburn BA; Sacks G; Hall KD; McPherson K; Finegood DT; Moodie ML; Gortmaker SL Lancet 2011, 378, 804–14. [PubMed: 21872749]

(8). Rosen ED; Walkey CJ; Puigserver P; Spiegelman BM Genes Dev. 2000, 14, 1293–307. [PubMed: 10837022]

(9). Moseti D; Regassa A; Kim WK Int. J. Mol. Sci 2016, 17, 124.

(10). Meng W; Liang X; Chen H; Luo H; Bai J; Li G; Zhang Q; Xiao T; He S; Zhang Y; Xu Z; Xiao B; Liu M; Hu F; Liu F Diabetes 2017, 66, 1198–1213. [PubMed: 28242620]

(11). Otani T; Mizokami A; Hayashi Y; Gao J; Mori Y; Nakamura S; Takeuchi H; Hirata M Cell. Signalling 2015, 27, 532–44. [PubMed: 25562427]

(12). Mishra AK; Lambright DG Biopolymers 2016, 105, 431–48. [PubMed: 26972107]

(13). van Dam TJ; Bos JL; Snel B Small GTPases 2011, 2, 4–16. [PubMed: 21686276]

(14). Ridley AJ Curr. Opin. Cell Biol 2015, 36, 103–12. [PubMed: 26363959]

(15). Villarroel-Campos D; Bronfman FC; Gonzalez-Billault C Cytoskeleton 2016, 73, 498–507. [PubMed: 27124121]

(16). Yang JQ; Kalim KW; Li Y; Zhang S; Hinge A; Filippi MD; Zheng Y; Guo FJ Allergy Clin. Immunol 2016, 137, 231–245.

(17). Rocha N; Payne F; Huang-Doran I; Sleigh A; Fawcett K; Adams C; Stears A; Saudek V; O'Rahilly S; Barroso I; Semple RK Sci. Rep 2017, 7, 17593. [PubMed: 29242557]

(18). Sordella R; Jiang W; Chen G-C; Curto M; Settleman J Cell 2003, 113, 147–158. [PubMed: 12705864]

(19). Strzelecka-Kiliszek A; Mebarek S; Roszkowska M; Buchet R; Magne D; Pikula S Biochim. Biophys. Acta, Gen. Subj 2017, 1861, 1009–1023. [PubMed: 28188861]

(20). Huang M; Wang Y Anal. Chem 2019, 91, 6233–6241. [PubMed: 30943010]

(21). Huang M; Qi TF; Li L; Zhang G; Wang Y Cancer Res. 2018, 78, 5431–5445. [PubMed: 30072397]

(22). Merkestein M; Laber S; McMurray F; Andrew D; Sachse G; Sanderson J; Li M; Usher S; Sellayah D; Ashcroft FM; Cox RD Nat. Commun 2015, 6, 6792. [PubMed: 25881961]

(23). Tang QQ; Otto TC; Lane MD Proc. Natl. Acad. Sci. U. S. A 2004, 101, 9607–11. [PubMed: 15210946]

(24). Huang M; Darvas M; Keene CD; Wang Y Anal. Chem 2019, 91, 12307–12314. [PubMed: 31460748]

(25). Pino LK; Searle BC; Bollinger JG; Nunn B; MacLean B; MacCoss MJ Mass Spectrom. Rev 2020, 39, 229. [PubMed: 28691345]

(26). Escher C; Reiter L; MacLean B; Ossola R; Herzog F; Chilton J; MacCoss MJ; Rinner O Proteomics 2012, 12, 1111–21. [PubMed: 22577012]

(27). Dani C; Smith AG; Dessolin S; Leroy P; Staccini L; Villageois P; Darimont C; Ailhaud GJ Cell Sci. 1997, 110, 1279–1285.

(28). Wennerberg K; Rossman KL; Der CJ J. Cell Sci 2005, 118, 843–6. [PubMed: 15731001]

(29). Grigoriadis AE; Heersche JN; Aubin JE J. Cell Biol 1988, 106, 2139. [PubMed: 3384856]

(30). Chen Q; Shou P; Zheng C; Jiang M; Cao G; Yang Q; Cao J; Xie N; Velletri T; Zhang X; Xu C; Zhang L; Yang H; Hou J; Wang Y; Shi Y Cell Death Differ. 2016, 23, 1128–39. [PubMed: 26868907]

(31). Ogino Y; Liang R; Mendonca DB; Mendonca G; Nagasawa M; Koyano K; Cooper LF J. Cell. Physiol 2016, 231, 568–75. [PubMed: 26205718]

(32). Skorobogatko Y; Dragan M; Cordon C; Reilly SM; Hung CW; Xia W; Zhao P; Wallace M; Lackey DE; Chen XW; Osborn O; Bogner-Strauss JG; Theodorescu D; Metallo CM; Olefsky JM; Saltiel AR Proc. Natl. Acad. Sci. U. S. A 2018, 115, 7819–7824. [PubMed: 29915037]

(33). Vernochet C; Mourier A; Bezy O; Macotela Y; Boucher J; Rardin MJ; An D; Lee KY; Ilkayeva OR; Zingaretti CM; Emanuelli B; Smyth G; Cinti S; Newgard CB; Gibson BW; Larsson NG; Kahn CR Cell Metab. 2012, 16, 765–76. [PubMed: 23168219]

(34). Ho AD; Wagner W; Franke W Cytotherapy 2008, 10, 320–30. [PubMed: 18574765]

(35). Reznikoff CA; Bertram JS; Brankow DW; Heidelberger C Cancer Res. 1973, 33, 3239–49. [PubMed: 4796800]

(36). Khayat G; Rosenzweig DH; Quinn TM Differentiation 2012, 83, 179–184. [PubMed: 22381625]

(37). Wang C; Liu Z; Huang X PLoS One 2012, 7, e32086. [PubMed: 22348149]

(38). Ji Y-H; Ji J-L; Sun F-Y; Zeng Y-Y; He X-H; Zhao J-X; Yu Y; Yu S-H; Wu W Mol. Cell. Proteomics 2010, 9, 550. [PubMed: 20008835]

(39). Jiang Y; Guo L; Xie L-Q; Zhang Y-Y; Liu X-H; Zhang Y; Zhu H; Yang P-Y; Lu H-J; Tang Q-QJ Proteome Res. 2014, 13, 1307–1314.

(40). Huang M; Wang Y Anal. Chem 2018, 90, 14551–14560. [PubMed: 30431262]

(41). Ang CS; Nice EC J. Proteome Res 2010, 9, 4346–55. [PubMed: 20684568]

(42). Percy AJ; Chambers AG; Yang J; Hardie DB; Borchers CH Biochim. Biophys. Acta, Proteins Proteomics 2014, 1844, 917–26.

(43). Meyers VE; Zayzafoon M; Douglas JT; McDonald JM J. Bone Miner. Res 2005, 20, 1858–66. [PubMed: 16160744]

(44). Li Q; Wang J; Wan Y; Chen D Biochem. Biophys. Res. Commun 2016, 471, 492–6. [PubMed: 26882978]

(45). Alto NM; Soderling J; Scott JD J. Cell Biol 2002, 158, 659–668. [PubMed: 12186851]

(46). Park M; Serpinskaya AS; Papalopulu N; Gelfand VI Curr. Biol 2007, 17, 2030–2034. [PubMed: 17997311]

(47). Yang D-C; Tsay H-J; Lin S-Y; Chiou S-H; Li M-J; Chang T-J; Hung S-C PLoS One 2008, 3, e1540. [PubMed: 18253488]

(48). Ries RJ; Zaccara S; Klein P; Olarerin-George A; Namkoong S; Pickering BF; Patil DP; Kwak H; Lee JH; Jaffrey SR Nature 2019, 571, 424–428. [PubMed: 31292544]

(49). Meyer KD; Patil DP; Zhou J; Zinoviev A; Skabkin M; Elemento O; Pestova TV; Qian S-B; Jaffrey SR Cell 2015, 163, 999–1010. [PubMed: 26593424]

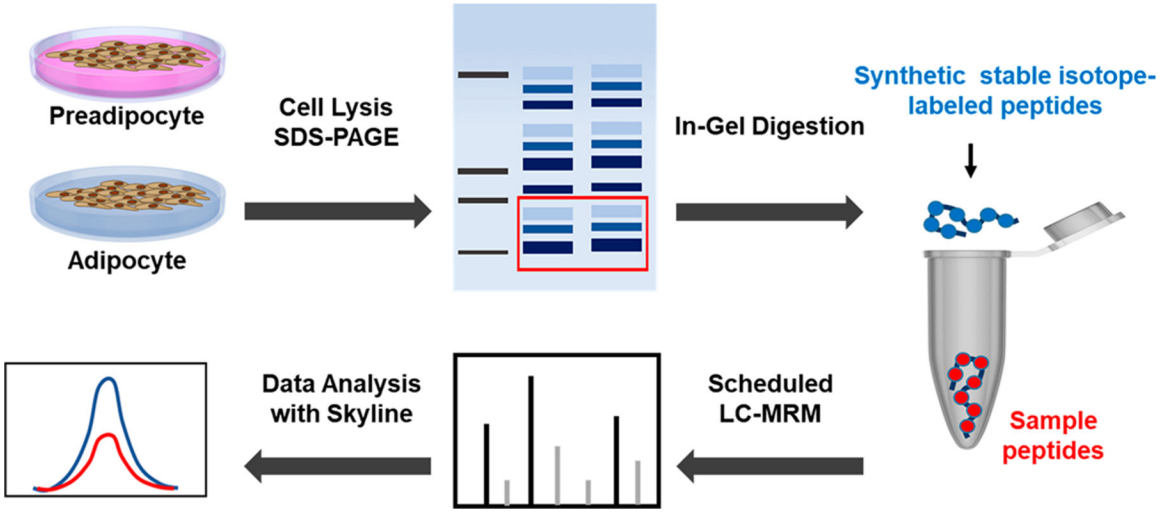

Figure 1.

Schematic diagram illustrating the scheduled MRM-based targeted proteomic workflow for assessing the alterations in small GTPase proteome during adipogenic differentiation. Cells were induced to differentiate to adipocytes and total lysates were collected for SDS-PAGE fractionation and in-gel tryptic digestion. Synthetic stable isotope-labeled peptides corresponding to 138 murine small GTPases were added to samples and the mixtures were subjected to scheduled MRM analysis. The results were analyzed with Skyline.

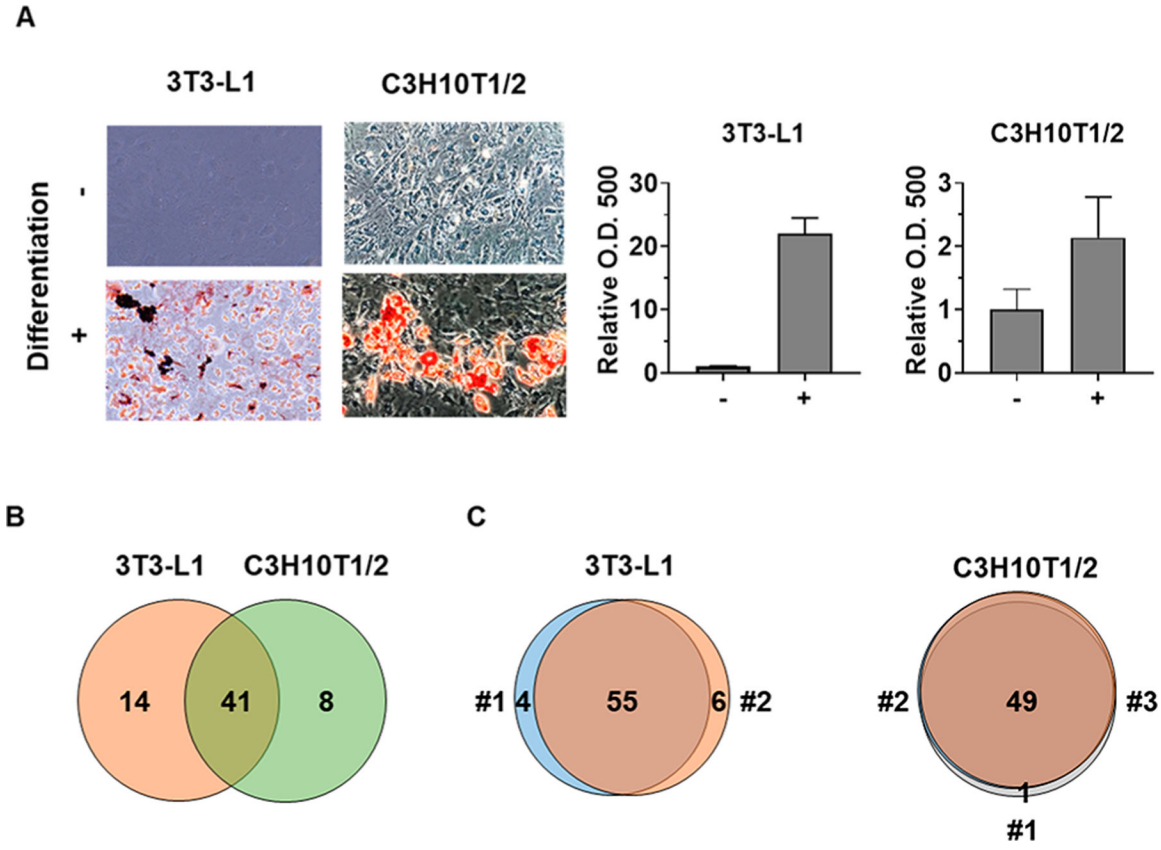

Figure 2.

Numbers of small GTPases quantified in 3T3-L1 and C3H10T1/2 murine cells during adipocyte differentiation. (A) 3T3-L1 murine fibroblast and C3H10T1/2 murine mesenchymal stem cells (−) were induced to differentiation into adipocytes (+). Adipogenesis efficiency was confirmed by Oil Red O staining. The lipid dye was later extracted and its UV absorbance at 500 nm was measured. The data represent the mean ± standard deviation (S.D.) of quantification results (n = 3). (B) Venn diagram showing the numbers of small GTPases in 3T3-L1 and C3H10T1/2 cells quantified with scheduled MRM analysis. (C) Venn diagrams showing the overlap of quantified small GTPases from the two biological replicates in 3T3-L1 cells and three biological replicates in C3H10T1/2 cells.

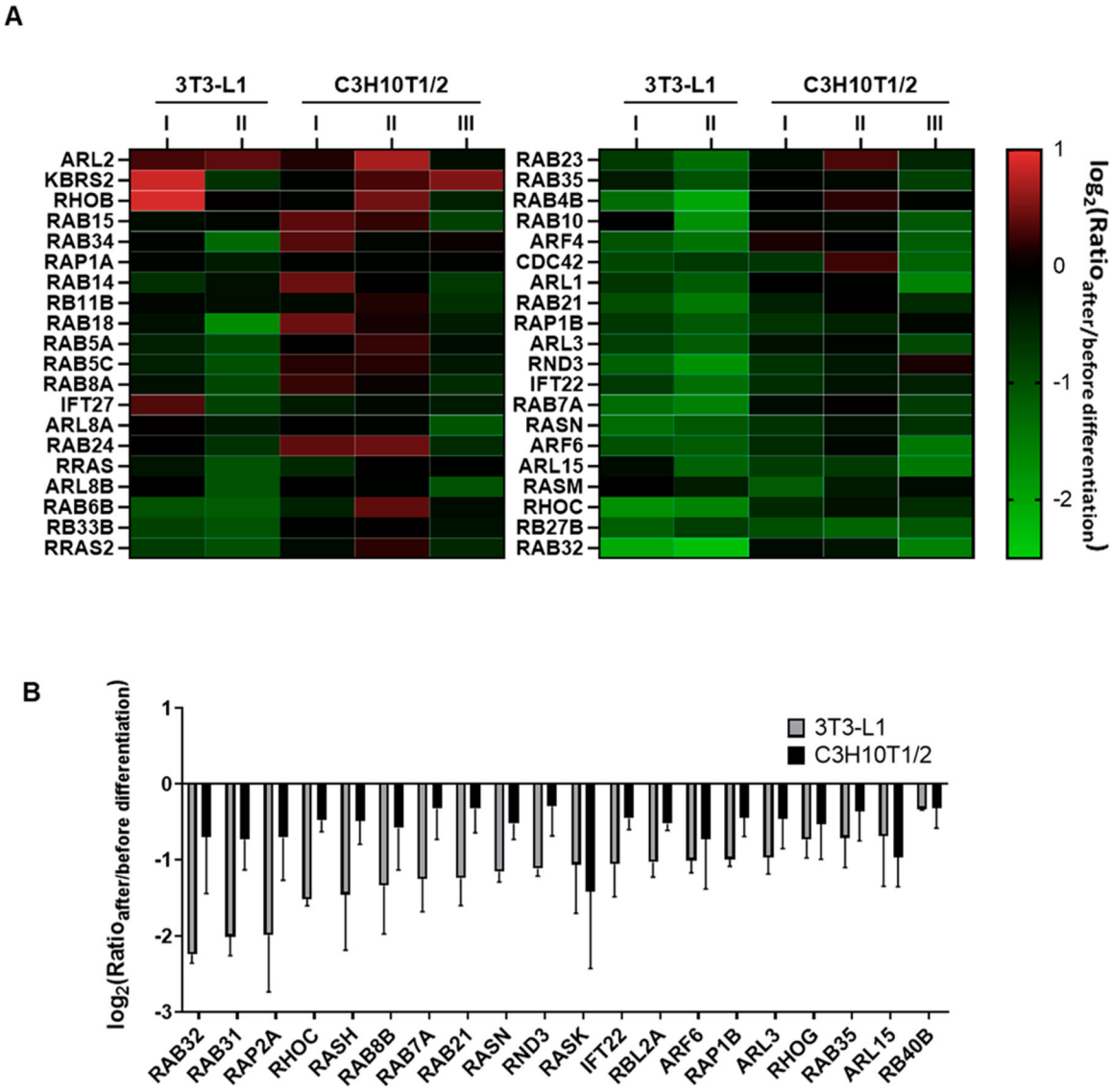

Figure 3.

Differentially expressed small GTPases upon adipocyte differentiation. (A) Heat map depicting the quantified small GTPases in 3T3-L1 and C3H10T1/2 cells upon differentiation. (B) Quantification data of top 20 differentially expressed small GTPases in 3T3-L1 and C3H10T1/2 cells. The data represent mean ± SD of results obtained from two and three biological replicates for 3T3-L1 and C3H10T1/2 cells, respectively.

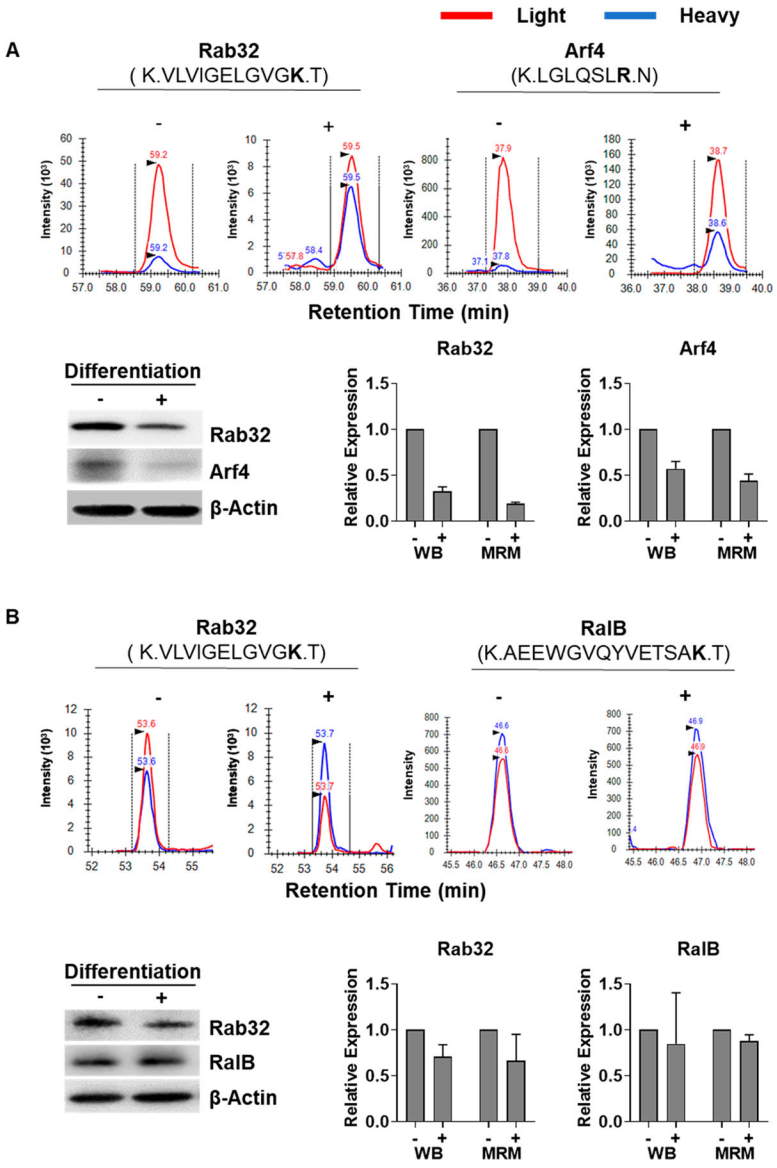

Figure 4.

Western blot validation of the quantification results obtained from scheduled MRM analysis. Shown are selected-ion chromatograms (upper panel) for monitoring tryptic peptides of representative small GTPases before (−) and after (+) differentiation of 3T3-L1 (A) and (B) C3H10T1/2 cells into adipocytes. The traces for the unlabeled peptides derived from cell lysates are shown in red and the corresponding traces for the spiked-in heavy isotope-labeled peptide are shown in blue. Western blot analysis (lower panel) was conducted to validate the MRM results of selected small GTPases. Band intensity of small GTPases was normalized against that of β-actin and further normalized against the ratio of the undifferentiated cells.

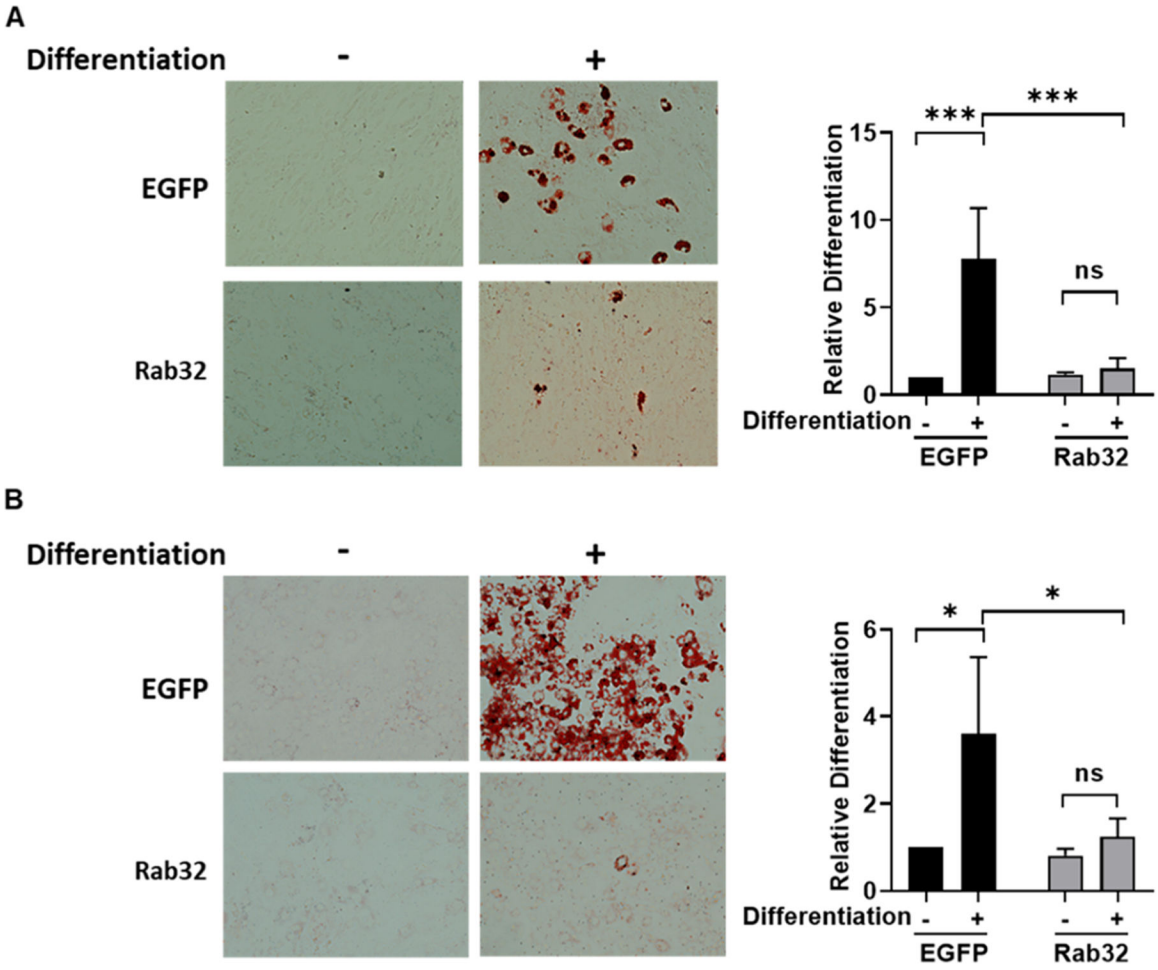

Figure 5.

Role of Rab32 in adipocyte differentiation. (A) 3T3-L1 and (B) C3H10T1/2 cells were transfected with control (EGFP) or EGFP-Rab32 plasmid followed by adipogenesis induction. The undifferentiated (−) and differentiated (+) cells were stained with Oil Red O and the adipogenesis efficiency was quantified by UV adsorption at 500 nm. The p values were calculated using two-tailed, unpaired Student's t-test: *, $0.01 < p < 0.05$; ***, $p < 0.001$; 'ns' designate not significant (i.e. $p > 0.05$).